Nonlinear photonic metasurfaces

Li, Guixin; Zhang, Shuang; Zentgraf, Thomas

DOI:
10.1038/natrevmats.2017.10

Document Version
Peer reviewed version

Citation for published version (Harvard):
Li, G, Zhang, S & Zentgraf, T 2017, 'Nonlinear photonic metasurfaces', *Nature Reviews Materials*, vol. 2, no. 5, 17010. https://doi.org/10.1038/natrevmats.2017.10

Nonlinear Photonic Metasurfaces

Guixin Li[1,2], Shuang Zhang[3], and Thomas Zentgraf[2]

[1]Department of Materials Science and Engineering, Southern University of Science and Technology, Shenzhen, China

[2]Department of Physics, University of Paderborn, Warburger Straße 100, D-33098 Paderborn, Germany

[3]School of Physics & Astronomy, University of Birmingham, Birmingham, B15 2TT, UK

Email: ligx@sustc.edu.cn; s.zhang@bham.ac.uk; thomas.zentgraf@uni-paderborn.de

Abstract: Compared to conventional optical elements, two dimensional photonic metasurfaces, consisting of arrays of antennas with subwavelength thickness, enable the manipulation of light-matter interaction on a more compact platform. Using metasurfaces, the polarization, phase and amplitude of light can be controlled by spatially variant meta-atoms with a subwavelength lateral resolution. Many exotic phenomena in linear optics such as imaging with ultrathin flat lenses, optical spin Hall Effect, highly efficient holography etc., have been successfully demonstrated. However, growing demand for integrating more functionalities into an optoelectronic circuit also relies on the availability of tailored nonlinear optical properties of metasurfaces. In this review, we will summarize the latest progress in optics with nonlinear photonic metasurfaces, particularly in device fabrication, nonlinear optical chirality, geometric Berry phase and wavefront engineering. Finally, we outlook several important applications of nonlinear photonic metasurfaces in optical switching and modulation, terahertz nonlinear optics, and quantum information processing.

Introduction:

Photonic metamaterials, consisting of artificial building blocks – the so-called 'meta-atoms', allow us to control light propagation in a way that cannot be realized by natural materials[1-4]. Linear optical properties such as effective permittivity and permeability as well as refractive index of metamaterials can be designed on demand by judiciously designing the material and geometry of each individual meta-atom. In such a way, the electromagnetic response of the meta-atom is no longer limited by its constituent chemical compounds. A plethora of novel optical phenomena such as negative refraction, superlensing, and cloaking have been demonstrated by particularly designed metamaterials[1-4]. However, both the difficulty of nanofabrication and large optical loss

of three dimensional metamaterials limit their practical applications in the optical regime.

With the recent development of photonic metasurfaces, a class of structured interfaces with spatially varying profiles of meta-atoms, it was shown that even a single layer of meta-atoms can be sufficient to modify the light propagation[1-3, 5-8]. The meta-atoms of two dimensional (2D) or quais-2D metasurfaces are metallic or dielectric resonators with remarkable capability of controlling the polarization, phase and amplitude of electromagnetic waves at subwavelength resolution. The two dimensional nature of ultrathin metasurfaces also allows for more compact optical devices and less optical loss compared to its bulk counterparts. Moreover, the deflection of light on a metasurface does not strongly rely on propagation effect compared to three dimensional metamaterials, consequently reducing the effect of dispersion. In addition, ultrathin metasurfaces are more compatible with state-of-the-art nanofabrication processes such as the complementary metal-oxide semiconductor technology. To some extent, the ultrathin metasurfaces that are utilizing the concept of the abrupt phase change of light across an interface have heralded a new era of "flat optics". At the early stage, many interesting optical phenomena such as extraordinary reflection and transmission, imaging by flat lenses, optical holography, optical spin Hall-Effect, and the generation of optical vortex beams have been investigated[9-20]. Meanwhile, the rapid progress of metasurface flat optics in linear optical regime is discussed in detailed in the several review articles[6-8]. Recently, much efforts have been dedicated to practical applications such as highly efficient metasurface holograms[21-24], high numerical aperture lenses[25-27], as well as well-defined generation and detection of spin and orbital angular momentum of light [28,29].

On the other hand, there has been an increasing demand on integrating multiple optical functionalities into a single compact chip design for ultrafast optical switching and optical information processing in both classical and quantum communications. For implementing such functionalities nonlinear optical effects play an important role[30, 31]. There is no doubt that the nonlinear optical response of meta-atoms will offer new degrees of freedom to the exceptional performance of linear photonic metasurfaces.

Nonlinearities have been used in a wide range of applications from X-ray to microwave regimes. Within the frame of this review, we will summarize the recent

progress of nonlinear photonic metasurfaces for visible to infrared wavelengths which have great potential for future on-chip applications. In addition, this review focusses on parametric nonlinear frequency conversion processes and optical switching and modulation on both periodic and aperiodic metasurfaces. First, we will introduce the basic principles of nonlinear optics, the material selection and symmetry considerations of nonlinear meta-atoms. Following that, the design of metasurfaces for realizing giant nonlinear chirality is discussed. Then, a new approach for precisely controlling the nonlinear optical phase is explained followed by a discussion of its application in nonlinear optical spin-orbit interaction, beam shaping and wavefront engineering of light. Finally, the recent progress in optical switching and modulation is summarized. We also outlook the remaining challenges and potential developments of nonlinear photonic metasurface in the near future.

1. Nonlinear Photonic Metasurfaces

Under the electric dipole approximation, the nonlinear optical response of a material to the electric field of light can be described by a power series expansion of the nonlinear material polarization[30, 31]:

$$\vec{P}^{NL} = \varepsilon_0(\chi^{(2)}\vec{E}\vec{E} + \chi^{(3)}\vec{E}\vec{E}\vec{E} + ...).$$

Whereas ε_0 is the vacuum permittivity, $\chi^{(2)}$ and $\chi^{(3)}$ are the second- and third-order nonlinear susceptibilities, respectively. The nonlinear material polarization acts as the source for new frequencies due to the mixing of the electric fields. The phase of the generated wave is determined by the susceptibility of the material and therefore linked to an intrinsic material parameter that generally cannot be altered in natural materials. In practical applications, the second- and third harmonic generations (SHG and THG) and FWM processes, which are related to $\chi^{(2)}$ and $\chi^{(3)}$, are routinely used for frequency conversion in laser systems. As schematically shown by the energy diagrams in Fig. 1, the SHG and THG involve a process that converts the frequency of a fundamental wave into nonlinear waves with doubled or tripled frequencies. FWM is a third-order nonlinear optical parametric process, whereby interactions between three fundamental photons (even with different energies) generate new frequencies of light. FWM has

broad applications in optical phase conjugation[32], optical switching and frequency comb generation[33] etc.

Selection of Nonlinear Optical Materials

Optical nonlinearities in the context of nanophotonics were first discussed for plasmonic nanostructures and later extended to metamaterials[34,35]. One key issue of nonlinear plasmonic and metamaterial devices is how to improve the efficiency of nonlinear optical processes and the strength of light-matter interaction. The metasurfaces discussed here refer to periodic or aperiodic extended photonic interfaces with subwavelength thickness, with the constituent plasmonic nanostructures acting as the meta-atoms (building blocks).

The nonlinear efficiency of plasmonic metamaterials is determined by both the macroscopic susceptibility of the meta-atoms and microscopic hyperpolarizability of the materials. At the level of constituent materials, noble metals such as gold, copper, and silver have been shown to exhibit strong second- and third-order nonlinear susceptibilities. The consideration of the excitation of localized surface plasmon polariton resonances can further lead to strong enhancement of the electromagnetic field in the vicinity of the meta-atoms. Therefore, the nonlinear optical response of plasmonic metamaterials can be tailored by designing the geometric properties of the meta-atoms (Fig. 2). However, the optical loss due to the absorption of the metals in three dimensional plasmonic metamaterials will ultimately affect their practical application in frequency conversion and light modulation. To this end, various physical mechanisms have been utilized to boost the nonlinear efficiency on a thin meta-atom platform. For example, it has been proposed that both the strong electric and magnetic resonances in plasmonic meta-atoms can improve the efficiency of SHG[36-48], THG[48-56], FWM[57-64]. An improved nonlinear optical efficiency of metasurfaces was obtained by using both organic and inorganic semiconductors in combination with the plasmonic meta-atom to form a composite metasurface[54,65]. By coupling intersubband transitions of multiple-quantum-well (MQW) semiconductor heterostructures with the plasmonic resonances of the meta-atoms, metal-MQW hybrid metasurfaces with a SHG efficiency several orders of magnitude higher than natural materials were recently demonstrated[65,66]. A different approach to realize enhanced nonlinearity in metasurfaces is based on the high third-order nonlinear susceptibility of π-conjugated

organic polymers. It has been demonstrated that the THG efficiency from such metal-organic hybrid metasurfaces can be two orders of magnitude stronger than that of the bare plasmonic metasurface[54]. All these enhancement effects utilize the strong field enhancement near the surface of the resonantly excited meta-atoms, leading to a strong nonlinear interactions with the materials in their proximity.

However, plasmonic metasurfaces have an obvious drawback: the low damage threshold under strong laser illumination limits the conversion efficiency. To circumvent this constraint, nonlinear metasurfaces made of pure dielectric or semiconductor materials have been exploited. Meanwhile, silicon metasurfaces (Fig. 2d) have been used to generate highly efficient THG signals employing both the electric[67] and the magnetic Mie resonances in the silicon meta-atoms[68]. In addition, an external static electric field can be mixed with the fundamental wave of the light to produce frequency doubled light in nonlinear optical materials with third-order susceptibility. In analogy to the SHG as a result of the second-order susceptibility this effect is called Electric Field Induced SHG (EFISHG)[69,70]. As there are less restrictions for third-order processes with respect to the spatial symmetry of the medium compared to the second-order process, it provides an interesting alternative in developing electro-optic nonlinear metasurfaces. Following this concept, the EFISHG effect with large modulation depth has been demonstrated using backward phase matching in plasmonic metasurfaces and strong exciton charging effects in monolayers of WSe_2[71-74]. Moreover, electrically tuneable plasmonic resonances in doped graphene metasurfaces can strongly interact with the fundamental wave to produced efficient SHG and THG[75,76] (Fig. 2e). Both the EFISHG effect and electrically controlled plasmonic resonances in meta-atoms open new exciting routes for developing tuneable nonlinear metasurface devices.

Symmetry of Metasurface Crystals

Symmetry plays a vital role for harmonic generations. In nonlinear optics, it is well known that the selection rules for frequency conversion processes are not only determined by the constituent ingredients of the materials but also by their spatial symmetry configuration of atomic crystal[30, 31]. Recent research has shown that the macroscopic symmetry of metasurfaces also leads to specific selection rules of nonlinear process as that of its microscopic counterpart[77,78]. The macroscopic symmetry

consists of both local symmetry of the individual meta-atom and the global symmetry of the meta-atoms lattice. In plasmonic metasurfaces, the localized plasmonic resonance of the meta-atom is very sensitive to its size, shape and dielectric environment. Therefore, the local symmetry is especially important for SHG (Fig. 2). In this regard, SHG has been extensively studied on plasmonic metasurfaces with locally broken inversion symmetry using split ring resonators[36]and L-shaped meta-atoms[37,40]. In addition, the multipole contribution to the SHG signal caused by retardation effects have to be considered when the size of the meta-atom is close to the wavelength of light[37]. It is not surprising that the phase, amplitude and polarization of the SHG signal can be well manipulated by properly engineering both the local and global symmetries of the metasurface. For example, SHG from noncentrosymmetric meta-atoms was enhanced by introducing passive elements which do not generate SHG by themselves[40]. Using a similar concept, the SHG efficiency of plasmonic metasurfaces can be greatly boosted by controlling coherent collective effects between meta-atoms or multi-resonances[46] which are supported by the individual meta-atoms (Fig. 2b). We note that the symmetry discussions here can also be applied to other even order nonlinear optical processes such as sum frequency generation or parametric down conversion.

Most work in nonlinear optics has focused on excitation with fundamental waves of linear polarization states. However, the circular polarization state representing the spin of photons plays an important role in optics, in particular in the emerging field of spin orbit coupling of light. In the early years of nonlinear optics, it was found that harmonic generation for circularly polarized waves also obeys certain selection rules which are related to both the order of the harmonic process and the rotational symmetry of the crystals[77,78]. For a circularly polarized fundamental wave propagating in a nonlinear medium, the total spin angular momentum of the incident photons and the spin angular momentum of the generated harmonic photon are generally different from each other, and this difference needs be provided by the crystal. For a crystal with m-fold symmetry, the transferred momentum p from the crystal to the generated photon is an integer multiple of the rotational symmetry order which leads to $p = m\hbar$. For n^{th} harmonic generation, the incident photon momentum is $n\hbar$, whereas the generated photon has spin momentum of $+\hbar$ (same spin as incident photons) or $-\hbar$ (opposite spin to the incident photons). Thus, the allowed orders n for harmonic generation are

$n = l(m \pm 1)$, where l being an arbitrary integer and the '±' signs corresponding to the same or opposite handiness of the circular polarization of the generated harmonic waves, respectively.

Recently, these selection rules have been successfully applied to nonlinear metasurfaces with various rotational symmetries[43,54] (Fig. 2a). By designing a metasurface crystal with three- and four-fold rotational symmetries, only circularly polarized SHG and THG with the opposite polarization state to the fundamental wave can be generated[43,54]. Interestingly, a three-fold rotational symmetric structure cannot generate a third harmonic wave for circularly polarized light, although this is possible for linear polarization states.

The nonlinear optical processes exert much less constraints on the design of two dimensional metasurfaces than on bulk metamaterial due to the relaxation of the phase matching condition along the propagation direction[35,84-86]. Like its three dimensional counterpart, metasurfaces have the ability to manipulate not only the linear but also the nonlinear optical responses by using suitable subwavelength meta-atoms. However, some features distinguish nonlinear optical metasurfaces from metamaterials. For example, phase-matching requirements[79-86], usually crucial for harmonic generation and FWM (Fig. 2f), can be dramatically relaxed. This is because the nonlinear process occurs only over a subwavelength thick layer. Under such condition, the phase mismatch does not play as an important role as that in conventional nonlinear optical crystal[30,31]. As the phase, amplitude and polarization of the nonlinear frequency conversion can be locally manipulated using spatially variant meta-atoms with sub-wavelength resolution, the nonlinear optical functionalities of metasurfaces obviously exceed most of the previously demonstrated plasmonic nanostructures.

2. Nonlinear Circular Dichroism

In the previous section we show that the symmetry of the meta-atoms can lead to a polarization dependent nonlinear response at the example of the selection rules for harmonic generation with circularly polarized light. The circular polarization states are also important for the interaction of light with chiral optical systems.

Chirality means that the mirror image of an object cannot be superposed onto the object itself. Optical chirality has been utilized for characterizing the symmetry of

chemical surfaces, biomolecule and optical crystals for long time. The two manifestations of optical chirality, optical activity (OA) and circular dichroism (CD), result from phase and absorption differences between left- and right-circularly polarized light passing through a chiral media. Usually, optical chirality is very weak in natural materials[87,88]. However, artificially engineered chiral metamaterials open new avenues for generating giant chiroptical responses by utilizing the strong plasmonic resonances[89-97]. Chiral metamaterials have been exploited for realization of negative refraction[89], infrared circular polarizers[93] and high sensitivity bio-sensing[94]. By the merit of its high sensitivity to the symmetry of physical interfaces, SHG based nonlinear optical chirality has become a mature technique for probing the chirality of chemical surfaces and biomolecules[98-101]. Nonlinear chirality in plasmonic metamaterials has attracted much attention recently. However, most of the reported nonlinear optical chirality is strongly correlated with the large linear optical chirality arising from the three dimensional nature of metamaterials, or from the extrinsic chirality under oblique incidence of the wave[102-108].

Nonlinear chiral metasurfaces are perfectly suited for studying nonlinear optical circular dichroism (Fig. 3a). They are not only easier to fabricate but also more compatible with physical interfaces of chiral molecules than bulk metamaterials (Fig. 3b). Although metasurfaces have intrinsic chirality in the linear optical regimes due to the asymmetric dielectric environment on the two sides of the meta-atoms, this kind of linear optical chirality is usually too weak to be reflected in the nonlinear optical processes. To avoid the extrinsic chirality from oblique incidence of light, it is also crucial to develop metasurfaces with extremely high nonlinear optical chirality for normally incident fundamental waves. Here, we summarize some of the recent progress in this area. For example, Valev et al. demonstrated that the nonlinear CD from a superchiral metasurface with a SHG-CD ($SHG-CD=(I_{LCP}^{2\omega}-I_{RCP}^{2\omega})/(I_{LCP}^{2\omega}+I_{RCP}^{2\omega})$) value of above 52% can be achieved by tuning the coupling between meta-atoms[109] (Fig. 3c). Later, Kolkowski et al. showed a nanoprism nonlinear metasurface with a SHG-CD value of up to 37%[110] (Fig. 3d). In their research, SHG-CD microscopy was used to read out the encoding character ‘R’ in the metasurface. More recently, Chen et al. revealed that giant nonlinear chirality can result from achiral Trisceli- (Fig. 3e) and Gammadion- type metasurfaces. The measured SHG-CD and THG-CD are up to 98% and 79%, respectively[111]. Compared to the giant nonlinear CD in above chiral

metasurfaces[109-111], the linear CD of the normally incident fundamental wave is almost unobservable in experiment. Therefore, the three dimensional metamaterial is not necessary to achieve the large optical CD. In addition, by combining strong extrinsic chirality with strong metamaterial optical nonlinearity such as in SRR metasurfaces, Ren et al. observed giant nonlinear OA which is much larger than that of lithium iodate crystals[112]. The nonlinear OA in SHG processes can also be manipulated as demonstrated by rotating metasurfaces with three-fold rotational symmetry along its rotational axis[111]. The concept of nonlinear chiral metasurfaces with giant nonlinear optical chirality enables more freedoms in designing chiroptical devices for both optoelectronics and bio-sensing applications.

3. Nonlinear Optical Phase Engineering

For normal media the chromatic dispersion of the refractive index prevents an efficient conversion from a fundamental wave to its harmonics. One way to circumvent this limitation is to control the local phase of nonlinear polarizability. In such a way the chromatic dispersive effects that result in a phase mismatch between fundamental and harmonic wave can be compensated, leading to dramatic enhancement of the frequency conversion efficiency[30,31]. Hence, in nonlinear optics, processes or methods that can locally and spatially engineer the phase of the nonlinear optical polarizability of the media are highly desired[79-81]. The most well-known scheme for spatially tailoring the phase of the nonlinearity is quasi-phase matching, which is often used in second-order nonlinear optical processes. Periodic electric poling in ferroelectric materials has been widely utilized to achieve quasi-phase matching condition which leads to highly efficient SHG and parametric down conversion[82,83]. To date, quasi-phase matching is particularly important for generating entangled photon pairs in a parametric down conversion process using periodically poled nonlinear crystals. Periodic poling has also been extended to two dimensional modulation of nonlinearities for generating vortex beams in harmonic generations.

Although conventional phase matching schemes have already achieved great success in practical applications, they also have certain drawbacks. For example, electric poling only generates binary phase states (zero and π) for the nonlinear polarizability. Such binary phase states can lead to undesired nonlinear optical processes. In addition, the domain size that can be fabricated by poled ferroelectric

materials is usually much larger than the wavelength of light, which can lead to unwanted diffraction orders. Solutions to the binary phase problem and the large domain sizes would result in higher efficiency and better controllability in nonlinear optical processes. Recently, the emergence of nonlinear metasurfaces provides novel solutions to circumvent these constraints by allowing a direct continuous and spatially variant tailoring of the nonlinear polarizability.

Nonlinear Geometric Berry Phase

The concept of poling for achieving a binary phase in the nonlinear material polarization has been recently applied to the design of nonlinear metasurface using 'split ring resonator' meta-atoms with sub-wavelength pixel size[45]. There, the mirror symmetry of the split ring resonator was used to reverse the sign of the effective nonlinear susceptibility $\chi^{(2)}$. By simply reversing the orientation of the split ring resonator a π phase shift of the local SHG radiations can be induced (Fig. 4a). Using this concept of generating a binary phase mask with meta-atoms for linearly polarized light, Segal et al. manipulated the diffraction angle and achieved a focusing effect for SHG signals. However, for more complex beam manipulation in a nonlinear process a continuous and spatially variant phase manipulation is certainly more beneficial.

In linear optics, it has been shown that a pure geometric Pancharatnam-Berry phase of the scattered light can be achieved by spatially rotating the orientation direction of the meta-atom at each site[113,114] (Fig. 4b and 4c). Such concept was first demonstrated by using surfaces with semiconductor microstructures[115,116]. One advantage of the Berry phase effect lies in the origin of the phase, which is purely geometric and therefore does not depend on structure sizes and inherent dispersive material/geometrical resonances. Inspired by the concept of the linear Berry phase element, a novel nonlinear photonic metasurface with continuously controllable phase of the local effective nonlinear polarizability was first demonstrated by Li et al[117].

Such a Berry phase in the nonlinear material polarization can be understood in a simple coordinate transformation process, as detailed in Ref. 117. For a circularly polarized fundamental wave propagating along the rotational axis of a meta-atom, the local effective nonlinear dipole moment can be expressed as: $p_\theta^{n\omega} = \alpha_\theta (E^\sigma)^n$, where

α_θ is the n^{th} harmonic nonlinear polarizability tensor of the meta-atom with orientation angle θ and E^σ is the electric field of fundamental wave. Here, $\sigma = \pm 1$ represents the left- or right- handed circular polarization, respectively. The nonlinear polarizabilities of the meta-atom can be expressed as: $\alpha^{n\omega}_{\theta,\sigma,\sigma} \propto e^{(n-1)i\sigma\theta}$ and $\alpha^{n\omega}_{\theta,-\sigma,\sigma} \propto e^{(n+1)i\sigma\theta}$ for harmonic generation with the same or the opposite circular polarization compared to that of the fundamental wave. The relative phase factors $(n-1)\sigma\theta$ and $(n+1)\sigma\theta$ of the nonlinear waves depend only on the geometric rotation of the meta-atom. Thus, through the novel concept of nonlinear geometric phases, two different continuous phases can be imprinted into the harmonic generation signals of opposite spins, which only rely on the orientation angle of the local dipole antenna. However, in certain applications, it is desired that a single nonlinear signal with well-defined phase is generated. To eliminate one of the harmonic signals, the selection rule in the preceding section can be exploited.

According to the selection rules of harmonic generations for circularly polarized fundamental waves (Fig. 5), a single meta-atom with *m*-fold rotational symmetry allows only for certain harmonic orders. Therefore, by choosing an appropriate local rotational symmetry of the meta-atom, it is possible to obtain a nonlinear signal of a single spin with well-defined nonlinear geometric Berry phase in the range from 0 to 2π (Table I). More importantly, the nanoantennas with rotational symmetry ($m \geq 3$) have an isotropic optical response in the linear optical regime. While the orientation angle controls the nonlinear phase for certain harmonic generation orders, it does not affect the linear optical response. In this way, the linear and the nonlinear optical properties of the rotationally symmetric antenna are decoupled from each other. Thus, Berry phase meta-atom elements provide a powerful yet simple route to control the nonlinear optical radiation with a phase-only metasurface without affecting the uniformity of the linear optical response.

The continuous phase control over the nonlinearity was experimentally demonstrated for second and third harmonic generations by using phase gradient metasurfaces consisting of plasmonic meta-atoms with three- and four-fold rotational symmetries (Fig. 5b-5d). For these two cases, the handedness of the circularly polarized SHG and THG is opposite to that of the circularly polarized fundamental wave, and the nonlinear waves possess a nonlinear geometric phase of $3\sigma\theta$ and $4\sigma\theta$, respectively.

Such a nonlinear geometric phase also exists for meta-atoms with lower rotational symmetries. As shown in Fig. 5b, meta-atoms with two-fold rotational symmetry allow generation of waves with nonlinear phase of $2\sigma\theta$ and $4\sigma\theta$ for the same and opposite circularly polarized THG signals[117]. Similarly, meta-atoms with one-fold rotational symmetry, such as split ring resonators, can be used for producing a phase shift of $\sigma\theta$ and $3\sigma\theta$ for left and right circularly polarized SHG, respectively[118] (Fig. 5a). Hence with restrictions by symmetry of the meta-atoms a continuous geometric Berry phase can be realized in various nonlinear orders by simple rotation of the meta-atom with respect to the laboratory frame.

Not only the phase but also the magnitude of the nonlinear radiation in the far field can be controlled by locally changing the nonlinear geometric Berry phase of each meta-atom. The concept is similar to a spatial light modulator that can change the diffraction efficiency of light in the linear optical regime. By properly designing the continuous phase of the effective nonlinear polarizability along the metasurface the total amount for harmonic generation into a certain direction can be controlled. The same concept can be used to precisely compensate the mismatch between fundamental wave and nonlinear wave in bulk metamaterials to achieve phase matched highly efficient frequency conversion.

The concept of an abrupt phase change for light passing a linear metasurface with V-shaped meta-atoms can be also used to manipulated the nonlinear optical phase for harmonic generations and FWM with linear polarization states. By finely adjusting the aspect ratio of nanocavity meta-atoms made of rectangular nanoapertures (like an inversed meta-atom), Almeida et al. showed that the nonlinear phase of FMW signals can be continuously tuned from zero to 2π[119] (Fig. 4d). Following this method, a continuous nonlinear phase can be obtained for harmonic generation as well. However, both the phase and amplitude of the nonlinear susceptibility strongly depend on the size and shape of each meta-atom. In addition, the transmission and reflection of the fundamental wave is not uniform for different meta-atoms, which might lead to limitations if the transmitted fundamental beam is needed for other functionalities.

Nonlinear Dynamic Berry Phase (Nonlinear rotational Doppler effect)

The nonlinear optical phase we discussed so far is mainly related to the geometric property of the meta-atom. It is also interesting to take into account temporal effects of a rotating metasurface. First, let us revisit the dynamic Berry phase in linear optics. For the light with spin angular momentum σ ($\sigma = \pm 1$)[120], corresponding to either left or right circular polarization states of light, will reverse its spin when it passes through a rotating half-wave plate at angular frequency of Ω. During that process the wave will accumulate a dynamic (time dependent) Berry phase of $\pm 2\Omega t$, whereas t is time. The dynamic phase change results in a frequency shift of $\pm 2\Omega$ of the transmitted light. The plus/minus sign corresponds to the sense of rotation with respect to the circular polarization, which results either in an increase or decrease of the frequency[121-126]. This frequency shift is usually called rotational Doppler shift.

In contrast to the successful demonstration of the dynamic Berry phase in linear optics, it was paid much less attention to the nonlinear counterpart. Following this concept, the nonlinear phase in harmonic generation from rotating metasurfaces should exhibit time dependent properties, which can be generalized as a nonlinear dynamic Berry phase. Until recently, Li et al. took into account the symmetry selection rules and conservation of spin angular momentum for circularly polarized harmonic generations together to propose a concrete protocol of how to demonstrate the dynamic Berry phase in nonlinear optics[127]. There it was shown that the nonlinear Berry phase of the harmonics generation light equals to $-(n \quad 1)s\sigma\Omega t$, where $s = \pm 1$ representing the rotational direction of metasurface, the sign corresponds to the same or opposite polarization state of n^{th} order of the harmonic generation process compared with the fundamental wave. Later, the authors experimentally observed the rotational Doppler effect through SHG from the rotating β-BBO crystal with three-fold rotational symmetry. Such rotational Doppler effect in nonlinear optics should appear in the same way for the harmonic generation of spinning metasurfaces.

Although the studies of the nonlinear optical phase on metasurfaces are at its early stage, the recent findings already demonstrate the distinct potential for altering nonlinear optical processes, which opens new routes for studying the nonlinear light-matter interaction in both space and time.

4. Nonlinear Optical Wavefront Engineering

Wavefront engineering of light has been successfully used for super resolution imaging, high-dimension entangled photons etc. Conventional optical components such as lenses, diffractive optical elements and spatial light modulators are widely used for shaping the wavefront of light. However, the thickness or pixel size of these conventional optical elements are usually larger than the wavelength of light, which inevitably limit the device miniaturization for on-chip optoelectronic applications. In contrast, ultrathin photonic metasurfaces show the exceptional ability of shaping the wavefront of light with sub-wavelength resolution. For example, various optical beams such as Airy and optical vortex beams have been realized using metasurfaces[128,129]. Computer generated holographic displays were also demonstrated using both plasmonic and dielectric metasurfaces operating at visible to near infrared wavelengths [13,14,19,21-24]. Optical efficiencies of ultrathin metasurface holograms above 80% were demonstrated, suggesting the strong potential for practical application[21]. Furthermore, spin dependent geometric Berry phase elements, with a full range of phase from zero to 2π, can be fabricated in a single lithography process. Therefore, the fabrication costs of metasurface holograms is much lower than that of conventional ones with the same phase steps.

Transferring the techniques of linear optical wavefront engineering to the nonlinear regime and combine them with concepts from nonlinear optics will open a new way in realizing compact and ultrafast optical devices. For example, nonlinear frequency conversion processes on ultrathin metasurface platforms can offer more freedom for wavefront engineering and mode conversion.

Binary Nonlinear Phase for Beam Shaping

One of the most famous wavefront engineering devices in nonlinear optics is the phase conjugate mirror which can exactly reflect the incident light back into its original direction but with the conjugated phase[130,131]. Since then, there has been growing interests of shaping nonlinear optical radiation. For example, nonlinear Raman-Nath diffraction of SHG can be controlled by encoding the binary phase into the ferroelectric crystal through electric field poling[132,133]. Later, the binary nonlinear optical phase from nonlinear microstructures were used to generate nonlinear Airy beams[134,136], which have important applications in optical micro-manipulation and generation of curved plasma channels. Recently, optical vortex beams for THG with a

binary intensity modulation of $\chi^{(3)}$ on metal-organic hybrid microstructure were demonstrated[135]. Moreover, by combining split ring resonator meta-atoms together with quantum wells, Wolf et al. showed that the coherent superposition of two subwavelength sources can be used to manipulate both the polarization and propagation trajectory of SHG radiation in the far field[137]. A binary nonlinear metasurface, consisting of split ring resonator meta-atoms, has been employed to realize second harmonic optical vortex and Airy beams[138] (Fig. 6a). It should be noted that these nonlinear beam shaping devices only utilizing two phase steps, which will inevitably introduce undesired diffraction effects due to the higher Fourier components of the nonlinear optical susceptibility.

Continuous Nonlinear Phase for Holography

A powerful application of nonlinear metasurfaces is the realization of nonlinear holograms. The recent developments of both geometric Berry phase and abrupt phase of nonlinear metasurfaces enable the continuous control over the phase change from zero to 2π for harmonic generations and FWM[117-119]. The full range nonlinear phase would not only provide better manipulation of the beam profile of nonlinear radiation but also remove the issue of twin image generation that is intrinsic to a binary phase modulation. Many interesting optical phenomena such as the nonlinear spin-orbit interaction of light, beam steering and light focusing have been experimentally demonstrated in harmonic generations and FWM processes. Combining the concept of nonlinear metasurface with mature holography optimisation techniques, one fundamental wave can be converted into multiple beam profiles or images by a single metasurface[139,140] (Fig. 6b and 6c). Thus, it is possible to encode multi-colour images and circular polarizations for different orders of harmonic generations by using nonlinear geometric phase elements. Recently, spin and wavelength multiplexed nonlinear metasurface holography has been experimentally demonstrated using the geometric Berry phase of the fundamental wave and the SHG signal from split ring resonators[140] (Fig. 6c). It was shown that the spin dependent nonlinear metasurface holograms can provide nondispersive and crosstalk-free post-selective channels for holographic multiplexing, which may have great potentials for multidimensional optical data storages and optical encryption.

5. Metasurface for Optical Switching and Modulation

A further important research area of nonlinear optics is related to optical switching and modulation for applications like optical interconnects, optical communication, high performance computing, and many other practical optical devices and systems. Several ultrafast switching technologies that are based on Kerr nonlinearity or free carrier nonlinearity in semiconductor materials have been developed. However, most of the semiconductor optical switches suffer from two photon absorption and relatively long free carrier lifetime[141-144]. Thus, the switching time is limited to tens of picoseconds. To achieve higher processing speed, other nonlinear optical materials with faster electronic third-order nonlinearity have been employed. For example, high switching speed optical modulator based on organic/silicon hybrid structure was proposed[141], in which the organic material has a large $\chi^{(3)}$ and does not suffer from the free carrier absorption of silicon.

Apart from semiconductor materials, ultrafast optical phenomena in noble metals have been extensively studied[145-149]. The efficient excitation of free electrons in metals can lead to strong Kerr-type nonlinearity, which corresponds to changes of the real and the imaginary parts of the refractive index. The fast relaxation processes of hot electrons in metals through electron-electron (a fast process with time scale of sub-picosecond) and electron-phonon scatterings (a process with time scale of picoseconds) opens important routes for fast optical switching. Plasmonic metamaterials, in which light-matter interaction is strongly localized in a subwavelength mode volume, extent the design opportunities for optical switches and modulators even more. The strong light localization in the plasmonic metamaterial is extremely important for enhancing the nonlinearity and the miniaturization of photonic devices[34]. Thus, plasmonic metamaterials or metasurfaces have high potential to overcome some of the obstacles in realizing ultrafast optical switches and modulators.

In the past decade important progress on all-optical ultrafast switching and modulation using plasmonic metamaterials and metasurfaces have been reported[150-167]. For example, MacDonald, et al. demonstrated ultrafast modulation of surface plasmon polaritons (SPP) on the femtosecond time scale by using the pump induced refractive index change of aluminium[150]; Rotenberg et al. realized ultrafast coupling of SPP to planar metal film[151]. By using the nonlocality of gold nanorod metamaterial, Wurtz et al. showed an ultrafast switch with high modulation ratio of 80% on a picosecond time scale[152]. Later, Ren et al. reported an optical switch based on a SRR metasurface with

modulation speed around 100 fs by using the ultrafast response of two-photon absorption in gold[154]. Recently, Harutyunyan et al. reported on the observation of anomalously strong changes to the ultrafast spectral responses of excited hot electrons in hybrid metal/oxide metasurfaces[157] (Fig. 7a). The study demonstrated that the combination of dielectric materials with the strong light matter interaction of plasmonic nanostructures can result in fast modulation responses with high modulation strength.

Therefore, particular attention was payed to the exploration of hybrid materials for optical switching applications. Most of the studies used third-order effects based on a large $\chi^{(3)}$ which results in changes of the complex refractive index of the material. Dani, et al. investigated the all-optical ultrafast switching and modulation properties of metal-silicon hybrid metamaterials. The authors achieved a 600 fs modulation speed and up to 60% modulation depth but the ultimate switching speed was limited by the lifetime of free carriers in amorphous silicon[158]. Strong optical modulation was also observed by using Plasmon enhanced Kerr nonlinearities in Indium-Tin-Oxide (ITO)[159] liquid crystal (LC) infiltrated fishnet metasurfaces[160]. Mediated by the exciton-LSPP coupling of plasmonic nanostructures with highly nonlinear dye molecules (J-aggregates), Vasa, et al. achieved a 10 fs timescale manipulation of the coupling energy, which represents an important step towards all-optical ultrafast plasmonic circuits[161].

For practical applications the optical loss and heating in plasmonic nanostructures are obstacles, which limit the performance. Utilizing dielectric metasurfaces and metamaterials could provide an alternative way for optical switching and modulation that inherently might by lossless and also lead to lower power consumption. Recently, magnetic resonances in silicon dielectric metasurfaces have been used to suppress the free carrier effect leading to an ultrafast switching time of 65 fs[162](Fig. 7b). Ultrafast plasmon modulation in the near- to mid-infrared range was demonstrated by intraband pumping of indium tin oxide (ITO) metamaterial[163]. Moreover, nanomechanical nonlinearity in both plasmonic and dielectric metadevices can also provide new concepts of designing all-optical modulators[164-169](Fig. 7c).Such devices can have low power consumption but the modulation speed is dramatically reduced compared to purely optical nonlinear effects.

Most concepts for optical modulators have in common that the light localization in metamaterial and metasurface devices can greatly reduce the all-optical switching time without suffering from a strong loss in modulation depth. By locally controlling

the nonlinear optical properties of meta-atom elements, it should be possible to well-defined tailor both the switching time and modulation depth of light signals. Recently, epsilon-near-zero materials such as indium tin oxide (ITO) or aluminium doped zinc oxide (AZO) also attract a lot of attention due to their large Kerr nonlinearity. The integration of these materials into metasurfaces may bring new opportunities for improving the performance of all-optical switching and modulation in the visible and near infrared spectral region[170,171].

Conclusions/perspective:

With this review we presented an overview of the rapid development of nonlinear photonic metasurface and its various optical functionalities in recent years. By manipulating the local and global symmetries of the meta-atom, efficient harmonic generation and FWM as well as their applications in optical chirality have been extensively studied for both plasmonic and dielectric metasurfaces. It has also been shown that the nonlinear geometric Berry phase and nonlinear abrupt phase for light passing a metasurface can be used for shaping the wavefront of nonlinear beams or for information multiplexing in holography. Currently, the optical efficiency of nonlinear metasurfaces is still very low. Therefore, a plethora of new materials and systems needs to be exploited in the future to boost the nonlinear frequency conversions efficiency further. A first approach in this direction was already explored by coupling meta-atoms to intersubband transitions of semiconductors[65]. With the further development of the functionality and performance of nonlinear metasurfaces we expect and increasing amount of applications and new research fields. For example:

The concept of nonlinear geometric Berry phase can be extended to high harmonic generation (HHG)[172-177]. By using symmetry controlled HHG from metasurface devices, both the polarization and wavefront of HHG orders could be well engineered. With the rapid progress of sub-cycle terahertz nonlinear optics, the rich physics of elementary excitations in semiconductors opens new routes for the study of quantum electronics[173,176]. We envision metasurfaces, made of semiconductor thin films or other two dimensional materials such as transition metal dichalcogenides, can be used for efficient HHG in terahertz nonlinear optics by the virtue of interband transition or plasmon resonance in its constituent materials.

Metasurfaces may also find potential application in quantum optics despite the combination of quantum optics with metasurfaces is largely unexplored so far. For example, entangled photons, generated by parametric down conversion processes in nonlinear optical crystals, plays a critical role in quantum optical communication[178]. While the polarization state of the entangled photons can be manipulated by using various phase matching schemes, the wavefront shaping of the photons for high dimensional information coding still relies on spatial light modulators. However, the size of spatial light modulators dramatically limits the on-chip quantum integration. Thus, the nonlinear quantum metasurface that features a combination of metasurface elements with conventional quantum photon sources for manipulating both the polarization state and the wave front of light is highly desirable in high dimensional quantum communications and could lead to novel integrated quantum optical devices.

It is obvious that there are great potentials of nonlinear photonic metasurface for applications that need to be exploited in future. If successful, multiple nonlinear optical functionalities could be integrated on an ultrathin photonic chip. All the dedicated efforts in this exciting area will undoubtedly benefit both fundamental physics and the practical applications of nonlinear metasurface in bio-sensing[177], imaging, classical and quantum optical information processing[178].

Acknowledgements

This work was financially supported by the Deutsche Forschungsgemeinschaft (Grant Nos. DFG TRR142/A05 and ZE953/7-1).

References:

1. Soukoulis, C. M. & Wegener, M. Past achievements and future challenges in the development of three-dimensional photonic metamaterials. *Nat. Photon*. **5,** 523–530 (2011).
2. Hess, O. et al. Active nanoplasmonic metamaterials. *Nat. Mater*. **11,** 573–584 (2012).
3. Zheludev, N. I. & Kivshar, Y.S. From metamaterials to metadevices. *Nat. Mater.* **11,** 917–924 (2012).
4. Pendry, J. B., Luo, Y. & Zhao, R. Transforming the optical landscape. *Science* **348,** 521–524 (2015).
5. Yu, N. et al. Light propagation with phase discontinuities: generalized laws of reflection and refraction. *Science* **334,** 333–337 (2011).
6. Kildishev, A. V., Boltasseva, A. & Shalaev, V. M. Planar photonics with metasurfaces. *Science* **339,** 1232009 (2013).
7. Meinzer, N., Barnes, W. L. & Hooper, I. R. Plasmonic meta-atoms and metasurfaces. *Nat. Photon*. **8,** 889–898 (2014).
8. Yu, N. & Capasso, F. Flat optics with designer metasurfaces. *Nat. Mater*. **13,** 139–150 (2014).
9. Ni, X., Emani, N. K., Kildishev, A., Boltasseva, V. A. & Shalaev, V. M. Broadband light bending with plasmonic nanoantennas. *Science* **335,** 427 (2012).
10. Sun, S. et al. Gradient-index meta-surfaces as a bridge linking propagating waves and surface waves. *Nat. Mater*. **11,** 426–431 (2012).
11. Chen, X. et al. Dual-polarity plasmonic metalens for visible light. *Nat. Commun.* **3,** 1198 (2012).
12. Chen, W. T. et al. High-efficiency broadband meta-hologram with polarization controlled dual images. *Nano Lett.* **14,** 225–230 (2013).
13. Ni, X., Kildishev, A. V. & Shalaev, V. M. Metasurface holograms for visible light. *Nat. Commun*. **4,** 2807 (2013).
14. Huang, L. et al. Three-dimensional optical holography using a plasmonic metasurface. *Nat. Commun*. **4,** 2808 (2013).
15. Li, G. et al. Spin-enabled plasmonic metasurfaces for manipulating orbital angular momentum of light. *Nano Lett.* **13,** 4148–4151(2013).

16. Yin, X. B., Ye, Z. L., Rho, J., Wang, Y. & Zhang, X. Photonic Spin Hall Effect at metasurfaces. *Science* **339,** 1405–1407 (2013).
17. Lin, D., Fan, P., Hasman, E. & Brongersma, M. L. Dielectric gradient metasurface optical elements. *Science* **345,** 298 (2014).
18. Khorasaninejad, M. & Crozier, K. B. Silicon nanofin grating as a miniature chirality-distinguishing beam-splitter. *Nat. Commun.* **5,** 5386 (2014).
19. Huang, Y. W. et al. Aluminum plasmonic multicolor meta-hologram. *Nano Lett.* **15,** 3122–3127 (2015).
20. Chong, K. E. et al. Polarization-independent silicon metadevices for efficient optical wavefront control. *Nano Lett*. **15,** 5369–5374 (2015).
21. Zheng, G. et al. Metasurface holograms reaching 80% efficiency. *Nat. Nanotech*. **10,** 308–312 (2015).
22. Arbabi, A., Horie, Y., Bagheri, M. & Faraon, A. Dielectric metasurfaces for complete control of phase and polarization with subwavelength spatial resolution and high transmission. *Nat. Nanotech*. **10,** 937–943 (2015).
23. Huang, L. et al. Broadband hybrid holographic multiplexing with geometric metasurfaces. *Adv. Mater*. **27,** 6444–6449 (2015).
24. Wen, D. et al. Helicity multiplexed broadband metasurface holograms. *Nat. Commun*. **6,** 8241 (2015).
25. Aieta, F., Kats, M. A., Genevet, P. & Capasso, F. Multiwavelength achromatic metasurfaces by dispersive phase compensation. *Science* **347,** 1342–1345 (2015).
26. Khorasaninejad, M. et al. Metalenses at visible wavelengths: Diffraction-limited focusing and subwavelength resolution imaging. *Science* **352,** 1190–1194 (2016).
27. Wang, Q. et al. Optically reconfigurable metasurfaces and photonic devices based on phase change materials. *Nat. Photon*. **10,** 60–65 (2016).
28. Maguid, E., Yulevich, I., Veksler, D., Kleiner, V., Brongersma, M. L. & Hasman, E. Photonic spin-controlled multifunctional shared-aperture antenna array. *Science* **352,** 1202–1206 (2016).
29. Chen, S., Cai, Y., Li, G., Zhang, S., & Cheah, K. W. Geometric metasurface fork gratings for vortex beam generation and manipulation. *Laser & Photon. Rev*. **2,** 322–326 (2016).
30. Shen, Y. R. *The Principles of Nonlinear Optics* (John Wiley, 1984).

31. Boyd, R. W. *Nonlinear Optics 3rd edn* (Academic Press, 2008).
32. Yariv, A. & Pepper, D. M. Amplified reflection, phase conjugation, and oscillation in degenerate four-wave mixing. *Opt. Lett*. **1,** 16–18 (1977).
33. Sefler G. A. & Kitayama, K. Frequency comb generation by Four-Wave Mixing and the role of fiber dispersion. *J. Lightwave Technol*. **16,** 1596 (1998).
34. Kauranen, M. & Zayats, A. V. Nonlinear plasmonics. *Nat. Photon*. **6,** 737–748 (2012).
35. Lapine, M., Shadrivov, I. V. & Kivshar, Y. S. Colloquium: Nonlinear metamaterials. *Rev. Mod. Phys*. **86,** 1093–1123 (2014).
36. Klein, M. W., Enkrich, C., Wegener, M. & Linden, S. *Science* **313,** 502–504 (2006).
37. Kujala, S., Canfield, B. K., Kauranen, M., Svirko, Y. & Turunen, J. Multipole interference in the second-harmonic optical radiation from gold nanoparticles. *Phys. Rev. Lett*. **98,** 167403 (2007).
38. Zhang, Y., Grady, N. K., Ayala-Orozco, C. & Halas, N. J. Three-dimensional nanostructures as highly efficient generators of second harmonic light. *Nano Lett.* **11,** 5519–5523 (2011).
39. Aouani, H. et al. Multiresonant broadband optical antennas as efficient tunable nanosources of second harmonic light. *Nano Lett*. **12,** 4997–5002 (2012).
40. Husu, H. et al. Metamaterials with tailored nonlinear optical response. *Nano Lett*. **12,** 673–677 (2012).
41. Linden, S., Niesler, F., Forstner, J., Grynko, Y., Meier, T. & Wegener, M. Collective effects in second-harmonic generation from split-ring-resonator arrays. *Phys. Rev. Lett*. **109,** 015502 (2012).
42. Czaplicki, R., Husu, H., Siikanen, R., Makitalo, J. & Kauranen, M. Enhancement of second-harmonic generation from metal nanoparticles by passive elements. *Phys. Rev. Lett*. **110,** 093902 (2013).
43. Konishi, K., Higuchi, T., Li, J., Larsson, J., Ishii, S. & Kuwata-Gonokami, M. Polarization-controlled circular second-harmonic generation from metal hole arrays with threefold rotational symmetry. *Phys. Rev. Lett*. **112,** 135502 (2014).

44. O'Brien, K. et al. Predicting nonlinear properties of metamaterials from the linear response. *Nat. Mater*. **14,** 379–383 (2015).
45. Segal, N., Keren-Zur, S., Hendler N. & Ellenbogen, T. Controlling light with metamaterial-based nonlinear photonic crystals. *Nat. Photon*. **9,** 180–184 (2015).
46. Celebrano, M. et al. Mode matching in multiresonant plasmonic nanoantennas for enhanced second harmonic generation. Nat. Nanotech. 10, 412–417 (2015).
47. Kruk, S. et al. Enhanced magnetic second-harmonic generation from resonant metasurfaces. *ACS Photon*. **2,** 1007–1012 (2015).
48. Sartorello, G. et al. Ultrafast optical modulation of second- and third-harmonic generation from cut-disk-based metasurfaces. *ACS Photon*. DOI: 10.1021/acsphotonics.6b00108 (2016).
49. Hanke, T., Krauss, G., Trautlein, D., Wild, B., Bratschitsch, R. & Leitenstorfer, A. Efficient nonlinear light emission of single gold optical antennas driven by few-cycle near-infrared pulses. *Phys. Rev. Lett*. **103,** 257404 (2009).
50. Utikal, T. et al. Towards the origin of the nonlinear response in hybrid plasmonic systems. *Phys. Rev. Lett*. **106,** 133901 (2011).
51. Liu, H. et al. Linear and nonlinear Fano resonance on two-dimensional magnetic metamaterials. *Phys. Rev. B* **84,** 235437 (2011).
52. Aouani, H., Rahmani, M., Navarro-Cía, M. & Maier, S. A. Third-harmonic upconversion enhancement from a single semiconductor nanoparticle coupled to a plasmonic antenna. *Nat. Nanotech*. **9,** 290–294 (2014).
53. Metzger, B., Schumacher, T., Hentschel, M., Lippitz, M. & Giessen, H. Third harmonic mechanism in complex plasmonic Fano structures. *ACS Photon*. **1,** 471–476 (2014).
54. Chen, S. M. et al. Symmetry selective third harmonic generation from plasmonic metacrystals. *Phys. Rev. Lett*. **113,** 033901 (2014).
55. Grinblat, G., Li, Y., Nielsen, M. P., Oulton, R. F. & Maier, S. A. Enhanced third harmonic generation in single germanium nanodisks excited at the anapole mode. *Nano Lett*. **16,** 4635–4640 (2016).

56. Smirnova, D. A., Khanikaev, A. B., Smirnov, Lev A. & Kivshar, Y. S. Multipolar Third-Harmonic Generation Driven by Optically Induced Magnetic Resonances. *ACS Photon*. **3,** 1468–1476 (2016).
57. Renger, J., Quidant, R., Van Hulst, N. & Novotny, L. Surface-enhanced nonlinear four-wave mixing. *Phys. Rev. Lett*. **104,** 046803 (2010).
58. Chen, P. Y. & Alù, A. Subwavelength imaging using phase-conjugating nonlinear nanoantenna arrays. *Nano Lett*. **11,** 5514–5518 (2011).
59. Palomba, S., Zhang, S., Park, Y., Bartal, G., Yin, X. & Zhang, X. Optical negative refraction by four-wave mixing in thin metallic nanostructures. *Nat. Mater*. **11,** 34–38 (2012).
60. Suchowski, H. et al. Phase mismatch-free nonlinear propagation in optical zero-index materials. *Science* **342,** 1223–1226 (2013).
61. Zhang, Y., Wen, F., Zhen, Y. R., Nordlander, P. & Halas, N. J. Coherent Fano resonances in a plasmonic nanocluster enhance optical four-wave mixing. *Proc. Natl Acad. Sci. USA* **110,** 9215–9219 (2013).
62. Rose, A., Powell, D. A., Shadrivov, I. V., Smith, D. R. & Kivshar, Y. S. Circular dichroism of four-wave mixing in nonlinear metamaterials. *Phys. Rev. B* **88,** 195148 (2013).
63. Suchowski, H., O'Brien, K., Wong, Z. J., Salandrino, A., Yin, X. & Zhang, X. Phase mismatch-free nonlinear propagation in optical zero-index materials. *Science* **342,** 1223–1226 (2013).
64. Simkhovich, B. & Bartal, G. Plasmon-enhanced four-wave mixing for super resolution applications. *Phys. Rev. Lett*. **112**, 056802 (2014).
65. Lee, J. et al. Giant nonlinear response from plasmonic metasurfaces coupled to intersubband transitions. *Nature* **511,** 65–69 (2014).
66. Nookula, N. et al. Ultrathin gradient nonlinear metasurface with a giant nonlinear response. *Optica* **3,** 283–288 (2016).
67. Shcherbakov, M. R. et al. Enhanced third-harmonic generation in silicon nanoparticles driven by magnetic response. *Nano Lett*. **14,** 6488–6492 (2014).
68. Yang, Y. et al. Nonlinear Fano-Resonant Dielectric Metasurfaces. *Nano Lett*. **15,** 7388–7393 (2015).
69. Terhune, R. W., Maker, P. D. & Savage, C. M. Optical harmonic generation in calcite. *Phys. Rev. Lett*. **8,** 404–406 (1962).

70. Lee, C., Chang, R. & Bloembergen, N. *Phys. Rev. Lett*. **18,** 167–170 (1967).
71. Cai, W., Vasudev, A. P. & Brongersma, M. L. Electrically controlled nonlinear generation flight with plasmonics. *Science 333*, 1720–1723 (2011).
72. Kang, L. et al. Electrifying photonic metamaterials for tunable nonlinear optics. *Nat. Commun*. **5,** 4680 (2014).
73. Lan, S. et al. Backward phase-matching for nonlinear optical generation in negative-index materials. *Nat. Mater*. **14,** 807–811 (2015).
74. Seyler, K. L. et al. Electrical control of second harmonic generation in a WSe2 monolayer transistor. *Nat. Nanotech*. **10,** 407–411 (2015).
75. Cox, J. D. & Garcia de Abajo, F. J. Electrically tunable nonlinear plasmonics in graphene nanoislands. *Nat. Commun*. **5,** 5725 (2014).
76. Cox, J. D. & Garcia de Abajo, F. J. Plasmon-enhanced nonlinear wave mixing in nanostructured graphene. *ACS Photon*. **2,** 306−312 (2015).
77. Burns, W. K. & Bloembergen, N. Third-harmonic generation in absorbing media of cubic or isotropic symmetry. *Phys. Rev. B* **4**, 3437–3450 (1971).
78. Bhagavantam, S. & Chandrasekhar, P. Harmonic generation and selection rules in nonlinear optics. *Proc. Indian Acad. Sci. A* **76,** 13–20 (1972).
79. Armstrong, J. A., Bloembergen, N., Ducuing, J. & Pershan, P. S. Interactions between light waves in a nonlinear dielectric. *Phys. Rev*. **127,** 1918–1939 (1962).
80. Patel, C. K. N. & Van Tran, N. Phase matched nonlinear interaction between circularly polarized waves. *Appl. Phys. Lett.* **15,** 189–191 (1969).
81. Shelton J. W. & Shen, Y. R. Phase matched third harmonic generation in cholesteric liquid crystals. *Phys. Rev. Lett*. **25,** 23–26 (1970).
82. Fejer, M. M., Magel, G. A., Jundt, D. H. & Byer, R. L. Quasi-phase-matched second harmonic generation: tuning and tolerances. *IEEE J. Quantum Electron*. **28,** 2631–2654 (1992).
83. Zhu, S. N., Zhu, Y. Y., Qin, Y. Q., Wang, H. F., Ge, C. Z. & Ming, N. B. Experimental realization of second harmonic generation in a Fibonacci optical superlattice of $LiTaO_3$. *Phys. Rev. Lett*. **78,** 2752–2755 (1997).
84. Zheludev, N. I. & Emel yanov, V. I. Phase matched Second harmonic generation from nanostructured metallic surfaces. *J. Opt. A Pure Appl. Opt*. **6,** 26–28 (2004).

85. Rose, A., Huang, D. & Smith, D. R. Controlling the second harmonic in a phase matched negative-index metamaterial. *Phys. Rev. Lett*. **107,** 063902 (2011).

86. Rose, A., Huang, D. & Smith, D. Nonlinear interference and unidirectional wave mixing in metamaterials. *Phys. Rev. Lett*. **110,** 063901 (2013).

87. Hazen, R. M. & Sholl, D. S. Chiral selection on inorganic crystalline surfaces. *Nat. Mater*. **2,** 367–374 (2003).

88. Ernst, K. H. Molecular chirality at surfaces. *Phys. Status Solidi B* **249,** 2057–2088 (2012).

89. Pendry, J. B. A chiral route to negative refraction. *Science* **306,** 1353–1355 (2004).

90. Kuwata-Gonokami, M. et al. Giant optical activity in quasi-two-dimensional planar nanostructures. *Phys. Rev. Lett*. **95,** 227401 (2005).

91. Rogacheva, A. V., Fedotov, V. A., Schwanecke, A. S. & Zheludev, N. I. Giant gyrotropy due to electromagnetic-field coupling in a bilayered chiral structure. *Phys. Rev. Lett*. **97,** 177401 (2006).

92. Plum, E., Fedotov, V. A. & Zheludev, N. I. Optical activity in extrinsically chiral metamaterial. *Appl. Phys. Lett*. **93,** 191911 (2008).

93. Gansel, J. K. et al. Gold helix photonic metamaterial as broadband circular polarizer. *Science* **325**, 1513–1515 (2009).

94. Hendry, E. et al. Ultrasensitive detection and characterization of biomolecules using superchiral fields. *Nat. Nanotech*. **5,** 783–787 (2010).

95. Zhang, S. et al. Photoinduced handedness switching in terahertz chiral metamolecules. *Nat. Commun*. **3**, 942 (2012).

96. Wu, C. et al. Spectrally selective chiral silicon metasurfaces based on infrared Fano resonances. *Nat. Commun*. **5,** 3892 (2014).

97. Kan, T. et al. Enantiomeric switching of chiral metamaterial for terahertz polarization modulation employing vertically deformable MEMS spirals. *Nat. Commun*. **6,** 8422 (2015).

98. Verbiest, T., Kauranen, M. & Persoons, A. Light-polarization-induced optical activity. *Phys. Rev. Lett*. **82,** 3601–3604 (1999).

99. Petralli-Mallow, T., Wong, T. M., Byers, J. D., Yee, H. I. & Hicks, J. M. Circular dichroism spectroscopy at interfaces: a surface second harmonic generation study. *J. Phys. Chem*. **97,** 1383–1388 (1993).

100. Byers, J. D., Yee, H. I. & Hicks, J. M. A second harmonic generation analog of optical rotatory dispersion for the study of chiral monolayers. *J. Chem. Phys*. **101,** 6233–6241 (1994).

101. Maki, J. J., Kauranen, M. & Persoons, A. Surface second-harmonic generation from chiral materials. *Phys. Rev. B* 51, 1425–1434 (1995).

102. Verbiest, T., Kauranen, M., Rompaey, Y. V. & Persoons, A. Optical activity of anisotropic achiral surfaces. *Phys. Rev. Lett*. 77, 1456–1459 (1996).

103. Valev, V. K. et al. Plasmonic ratchet wheels: switching circular dichroism by arranging chiral nanostructures. *Nano Lett*. **9,** 3945–3948 (2009).

104. Valev, V. K. et al. Asymmetric optical second-harmonic generation from chiral G-shaped gold nanostructures. *Phys. Rev. Lett*. **104,** 127401 (2010).

105. Belardini, A., Larciprete, M. C., Centini, M., Fazio, E. & Sibilia, C. Circular dichroism in the optical second-harmonic emission of curved gold metal nanowires. *Phys. Rev. Lett*. **107,** 257401 (2011).

106. Huttunen, M. J., Bautista, G., Decker, M., Linden, S., Wegener, M. & Kauranen, M. Nonlinear chiral imaging of subwavelength-sized twisted-cross gold nanodimers. *Opt. Mater. Express* **1,** 46–56 (2011).

107. Rose, A., Powell, D. A., Shadrivov, I. V., Smith, D. R. & Kivshar, Y. S. Circular dichroism of four-wave mixing in nonlinear metamaterials. *Phys. Rev. B* **88,** 195148 (2013).

108. Rodrigues, S. P., Lan, S., Kang, L., Cui, Y. & Cai, W. Nonlinear imaging and spectroscopy of chiral metamaterials. *Adv. Mater*. **26,** 6157–6162 (2014).

109. Valev, V. K. et al. Nonlinear superchiral meta-surfaces: Tuning chirality and disentangling non-reciprocity at the nanoscale. *Adv. Mater*. **26,** 4074–4081 (2014).

110. Kolkowski, R., Petti, L., Rippa, M., Lafargue, C. & Zyss, J. Octupolar plasmonic meta-molecules for nonlinear chiral watermarking at subwavelength scale. *ACS Photon*. **2,** 899–906 (2015).

111. Chen, S. et al. Giant nonlinear optical activity of achiral origin in planar metasurfaces with quadratic and cubic nonlinearities. *Adv. Mater*. **28,** 2992–2999 (2016).

112. Ren, M., Plum, E., Xu, J. & Zheludev, N. I. Giant nonlinear optical activity in a plasmonic metamaterial. *Nat. Commun*. **3,** 833 (2012).

113. Pancharatnam, S. Generalized theory of interference, and its applications. Part I. Coherent pencils. *Proc. Indian Acad. Sci. Sect. A* **44,** 247–262 (1956).

114. Berry, M. V. Quantal phase factors accompanying adiabatic changes. *Proc. R. Soc. London Ser. A* **392,** 45–57(1984).

115. Bornzon, Z., Biener, G., Kleiner, V. & Hasman, E. Space-variant Pancharatnam Berry phase optical elements with computer-generated subwavelength gratings. *Opt. Lett*. **27,** 1141–1143 (2002).

116. Hasman, E., Kleiner, V., Biener, G. & Niv, A. Polarization dependent focusing lens by use of quantized Pancharatnam–Berry phase diffractive optics. *Appl. Phys. Lett*. **82,** 328–330 (2003).

117. Li, G. et al. Continuous control of the nonlinearity phase for harmonic generations. *Nat. Mater*. **14,** 607–612 (2015).

118. Tymchenko, M. et al. Gradient nonlinear Pancharatnam-Berry metasurfaces. *Phys. Rev. Lett*. **107,** 207403 (2016).

119. Almeida, E., Shalem, G. & Prior, Y. Subwavelength nonlinear phase control and anomalous phase matching in plasmonic metasurfaces. *Nat. Commun*. **7,** 10367 (2016).

120. Poynting, J. H. The wave motion of a revolving shaft, and a suggestion as to the angular momentum in a beam of circularly polarised light. *Proc. R. Soc. Lond. A* **82,** 560–567 (1909).

121. Beth, R. A. Mechanical detection and measurement of the angular momentum of light. *Phys. Rev.* **50,** 115–125 (1936).

122. Allen, P. J. A radiation torque experiment. *Am. J. Phys.* **34,** 1185–1192 (1966).

123. Garetz, B. A. & Armold, S. Variable frequency shifting of circularly polarized laser radiation via a rotating half-wave retardation plate. *Opt. Commun.* **31,** 1–3 (1979).
124. Garetz, B. A. Angular Doppler effect. *J. Opt. Soc. Am.* **71,** 609–611 (1980).
125. Simon, R., Kimble, H. J. & Sudarshan, E. C. G. Evolving geometric phase and its dynamical manifestation as a frequency shift: an optical experiment. *Phys. Rev. Lett.* **61,** 19–22 (1988).
126. Dholakia, K. An experiment to demonstrate the angular Doppler effect on laser light. *Am. J. Phys.* **66,** 1007–1010 (1998).
127. Li, G., Zentgraf, T. & Zhang, S. Rotational Doppler effect in nonlinear optics. *Nat. Phys*. **12,** 736-740 (2016).
128. Li, L., Li, T., Wang, S. M., Zhang, C. & Zhu, S. N. Plasmonic airy beam generated by in-plane diffraction. *Phys. Rev. Lett*. **107,** 126804 (2011).
129. Dolev, I., Epstein, I. & Arie, A. Surface-plasmon holographic beam shaping. *Phys. Rev. Lett*. **109,** 203903 (2012).
130. Gabor, D. A new microscopic principle. *Nature* **161,** 777–778 (1948).
131. Pendry, J. B. Time reversal and negative refraction. *Science* **332,** 71–73 (2008).
132. Berger, V. Nonlinear photonic crystals. *Phys. Rev. Lett.* **81,** 4136–4139 (1998).
133. Broderick, N. G. R., Ross, G. W., Offerhaus, H. L., Richardson, D. J. & Hanna, D. C. Hexagonally poled lithium niobate: a two-dimensional nonlinear photonic crystal. *Phys. Rev. Lett*. **84,** 4345–4348 (2000).
134. Ellenbogen, T., Voloch-Bloch, N., Ganany-Padowicz, A. & Arie, A. Nonlinear generation and manipulation of Airy beams. *Nat. Photon*. **3,** 395–398 (2009).
135. Li, G., Chen, S., Cai, Y., Zhang, S. & Cheah, K. W. Third harmonic generation of optical vortices using holography based gold-fork microstructure. *Adv. Opt. Mater*. **2,** 389–393 (2014).
136. Hong, X., Yang, B., Zhang, C., Qin, Y. Q. & Zhu, Y. Y. Nonlinear volume holography for wave-front engineering. *Phys. Rev. Lett*. **113,** 163902 (2014).
137. Wolf, O. et al. Phased-array sources based on nonlinear metamaterial nanocavities. *Nat. Commun*. **6,** 7667 (2015).

138. Keren-Zur, S., Avayu, O., Michaeli, L. & Ellenbogen, T. Nonlinear beam shaping with plasmonic metasurfaces. *ACS Photon*. **3,** 117–123 (2016).
139. Almeida, E., Bitton, O. & Prior, Y. Nonlinear metamaterials for holography. *Nat. Commun*. **7,** 12533 (2016).
140. Ye, W. et al. Spin and wavelength multiplexed nonlinear metasurface holography. *Nat. Commun*. **7,** 11930 (2016).
141. Koos, C. et al. All optical high speed signal processing with silicon organic hybrid slot waveguides. *Nat. Photon*. **3,** 216–219 (2009).
142. Nozak, et al. Sub-femtojoule all-optical switching using a photonic-crystal nanocavity. *Nat. Photon*. **4,** 477–483 (2010).
143. Reed, G. T., Mashanovich, G., Gardes, F. Y. & Thomson, D. J. Silicon optical modulators. *Nat. Photon*. **4,** 518–526 (2010).
144. Leuthold, J. Koos, C. & Freude, W. Nonlinear silicon photonics. *Nat. Photon*. **4,** 535–544 (2010).
145. Groeneveld, R. H. M. Sprik, R. & Lagendijk, A. Ultrafast relaxation of electrons probed by surface plasmons at a thin silver film. *Phys. Rev. Lett*. **12,** 784–787 (1990).
146. Fann, W. S., Storz, R., Tom, H. W. K. & Bokor, J. Direct measurement of nonequilibrium electron energy distributions in subpicosecond laser heated gold films. *Phys. Rev. Lett*. **68,** 2834–2837 (1992).
147. Fatti, N. D., Bouffanais, R., Vallee, F. & Flytzanis, C. Nonequilibrium electron interactions in metal films. *Phys. Rev. Lett*. **81,** 922–925 (1998).
148. Lamprecht, B., Krenn, J. R., Leitner, A. & Aussenegg, F. R. Resonant and off-resonant light driven plasmons in metal nanoparticles studied by femtosecond resolution third harmonic generation. *Phys. Rev. Lett*. **83,** 4421–4424 (1999).
149. Guo, C. L., Rodriguez, G. & Taylor, A. J. Ultrafast dynamics of electron thermalization in gold. *Phys. Rev. Lett*. **86,** 1638–1641 (2001).
150. MacDonald, K. F., Samson, Z. L., Stockman, M. I. & Zheludev, N. I. Ultrafast active plasmonics. *Nat. Photon*. **3,** 55–58 (2009).
151. Rotenberg, N., Betz, M. & van Driel, H. M. Ultrafast all-optical coupling of light to surface plasmon polaritons on plain metal surfaces. *Phys. Rev. Lett*. **105,** 017402 (2010).

152. Wurtz, G. A. et al. Designed ultrafast optical nonlinearity in a plasmonic nanorod metamaterial enhanced by nonlocality. *Nat. Nanotech*. **6,** 106–110 (2011).
153. Neira, A. D., Olivier, N., Nasir, M. E., Dickson, W., Wurtz, G. A. & Zayats, A. V. Eliminating material constraints for nonlinearity with plasmonic metamaterials. *Nat. Commun*. **6,** 7757 (2015).
154. Ren, M. et al. Nanostructured plasmonic medium for terahertz bandwidth all-optical switching. *Adv. Mater*. **23,** 5540–5544 (2011).
155. Lu, C. et al. An actively ultrafast tunable giant slow-light effect in ultrathin nonlinear metasurfaces. *Light: Sci. & Appl*. **4,** e302 (2015).
156. Valente, J., Ou, J. Y., Plum, E., Youngs, I. J. & Zheludev, N. I. A magneto-electro-optical effect in a plasmonic nanowire material. *Nat. Commun*. **6,** 7021 (2015).
157. Harutyunyan, H. Anomalous ultrafast dynamics of hot plasmonic electrons in nanostructures with hot spots. *Nat. Nanotech*. **10,** 770–774 (2015).
158. Dani, K. M., Ku, Z., Upadhya, P. C., Prasankumar, R. P., Brueck, S. R. J. & Taylor, A. J. Sub-picosecond optical switching with a negative index metamaterial. *Nano Lett*. **9,** 3565–3569 (2009).
159. Abb, M., Wang, Y., de Groot C. H. & Muskens, O. L. Hotspot-mediated ultrafast nonlinear control of multifrequency plasmonic nanoantennas. *Nat. Commun*. **5,** 4869 (2014).
160. Minovich, A. et al. Liquid crystal based nonlinear fishnet metamaterials. *Appl. Phys. Lett*. **100,** 121113 (2012).
161. Vasa, P. et al. Real-time observation of ultrafast Rabi oscillations between excitons and plasmons in metal nanostructures with J-aggregates. *Nat. Photon*. **7,** 128−132 (2013).
162. Shcherbakov, M. R. et al. Ultrafast All-Optical Switching with Magnetic Resonances in Nonlinear Dielectric Nanostructures. *Nano Lett*. **15,** 6985−6990 (2015).
163. Guo, P., Schaller, R. D., Ketterson, J. B. & Chang, R. P. H. Ultrafast switching of tunable infrared plasmons in indium tin oxide nanorod arrays with large absolute amplitude. *Nat. Photon*. **10,** 267–273 (2016).
164. Lapine, M. et al. Structural tunability in metamaterials. *Appl. Phys. Lett*. **95,** 084105 (2009).

165. Tao, H. et al. Reconfigurable terahertz metamaterials. *Phys. Rev. Lett*. **103,** 147401 (2009).
166. Pryce, I. M., Aydin, K., Kelaita, Y. A., Briggs, R. M. & Atwater, H. A. Highly strained compliant optical metamaterials with large frequency tunability. *Nano Lett*. **10,** 4222–4227 (2010).
167. Ou, J. Y., Plum, E., Zhang, J. & Zheludev, N. I. Giant nonlinearity of an optically reconfigurable plasmonic metamaterial. *Adv. Mater*. **28,** 729–733 (2015).
168. Karvounis, A., Ou, J. Y., Wu, W., MacDonald, K. F. & Zheludev, N. I. Nano-optomechanical nonlinear dielectric metamaterials. Appl. Phys. Lett. 107, 191110 (2015).
169. Zheludev, N. I. & Plum, E. Reconfigurable nanomechanical photonic metamaterials. *Nat. Nanotech*. **11,** 16-22 (2016).
170. Zahirul Alam, M., De Leon I. & Boyd, R. W. Large optical nonlinearity of indium tin oxide in its epsilon-near-zero region. *Science* **352,** 795–797 (2016).
171. Caspani, L. et al. Enhanced nonlinear refractive index in ε-Near-Zero materials. *Phys. Rev. Lett*. **116,** 233901 (2016).
172. Zürch, M., Kern, C., Hansinger, P., Dreischuh, A. & Spielmann, Ch. Strong-field physics with singular light beams. *Nat. Phys*. **8,** 743–746 (2012).
173. Fleischer, A., Kfir, O., Diskin, T., Sidorenko, P. & Cohen, O. Spin angular momentum and tunable polarization in high-harmonic generation. *Nat. Photon.* **8,** 543–549 (2014).
174. Schubert, O., Hohenleutner, M., Langer, F., Urbanek, B., Lange, C., Huttner, U., Golde, D., Meier, T., Kira, M., Koch, S. W. & Huber, R. Sub-cycle control of terahertz high-harmonic generation by dynamical Bloch oscillations. *Nat. Photon*. **8,** 119–123 (2014).
175. Hickstein, D. D. et al. Noncollinear generation of angularly isolated circularly polarized high harmonics. *Nat. Photon.* **9,** 743–750 (2015).
176. Hohenleutner, M. et al. Real-time observation of interfering crystal electrons in high-harmonic generation. *Nature* **523,** 572–575 (2015).

177. Baykusheva, D., Ahsan, M. S., Lin, N. & Wörner, H. J. Bicircular high-harmonic spectroscopy reveals dynamical symmetries of atoms and molecules. *Phys. Rev. Lett*. **116,** 123001 (2016).
178. Walmsley, I. A. Quantum optics: science and technology in a new light. *Science* **348,** 525– 530 (2015).

Figures

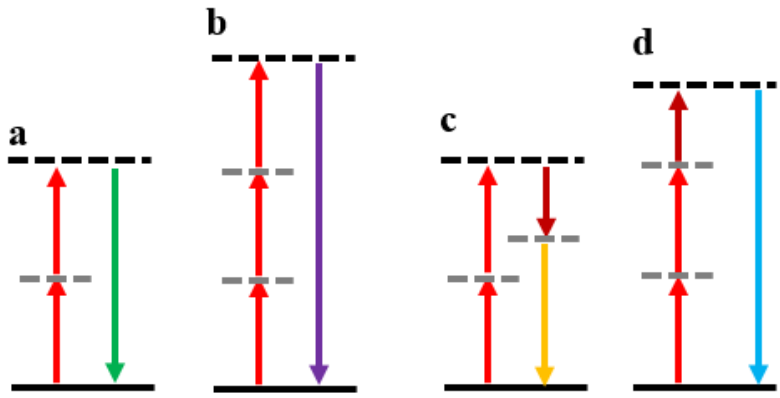

Figure 1| Schematic energy diagrams of important nonlinear optical processes. Fundamental photons of identical or different energy can lead to virtual transitions that result in the generation of new frequencies. The solid and dashed lines represent electronic and virtual levels for the excitation of the material polarization, respectively. a, Second harmonic generation (SHG). b, Third harmonic generation (THG). c and d, Nondegenerate four-wave mixing (FWM).

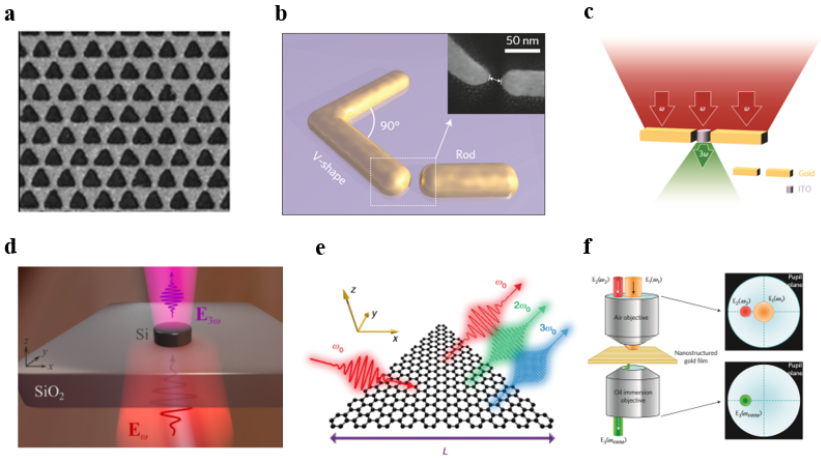

Figure 2| Nonlinear photonic metasurfaces. a, b, Plasmonic metasurfaces for SHG (ref. 43, 46), the meta-atoms have in common the locally broken inversion symmetry. c, d, Plasmonic (ref. 52) and dielectric (ref. 67) metasurfaces for THG. e, Electrically tunable SHG and THG in graphene nano-islands (ref. 75). The nanostructured graphene surface acts as an assembly of meta-atoms. f, Optical negative refraction by FWM from metallic nanostructures (ref. 59).

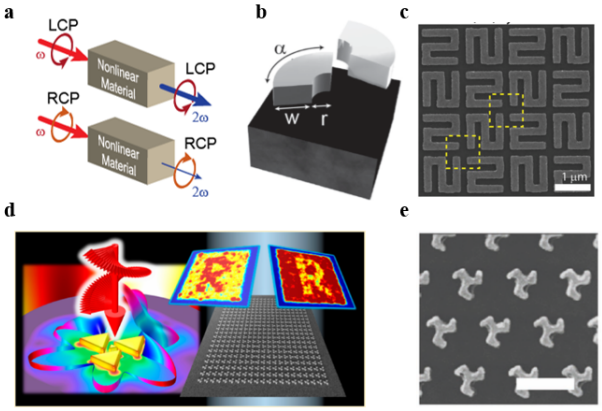

Figure 3| Nonlinear optical circular dichroism. a, Schematic illustration of nonlinear circular dichroism for second harmonic generation (SHG-CD). b, Three dimensional nonlinear chiral metamaterial with simultaneously strong linear and nonlinear chirality (ref. 108). c, Scanning electron microscopy image of superchiral metasurface (ref. 109). d, Plasmonic metasurface for nonlinear chiral watermarking (ref. 110). The meta-atoms are used to encode an image into the SHG signal. e, Trisceli-type chiral metasurface with quadratic nonlinearity showing strong nonlinear chirality for normal light incidence, scale bar: 500 nm (ref. 111).

Harmonic orders	$\sigma(n\omega)$	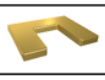 C1	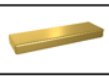 C2	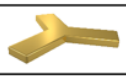 C3	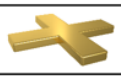 C4
n=1	+				
	-	$2\theta\sigma$	$2\theta\sigma$		
n=2	+	$\theta\sigma$			
	-	$3\theta\sigma$		$3\theta\sigma$	
n=3	+	$2\theta\sigma$	$2\theta\sigma$		
	-	$4\theta\sigma$	$4\theta\sigma$		$4\theta\sigma$
n=4	+	$3\theta\sigma$		$3\theta\sigma$	
	-	$5\theta\sigma$			
n=5	+	$4\theta\sigma$	$4\theta\sigma$		$4\theta\sigma$
	-	$6\theta\sigma$	$6\theta\sigma$	$6\theta\sigma$	

Table 1| Nonlinear Geometric Berry Phase. The order of the nonlinear process and the rotational symmetry group determine the phase of the nonlinear wave during the harmonic generation processes. n = 1…5: order of harmonic generation; C1-C4: number of the rotational symmetry of the meta-atom; θ: relative orientation angle of the meta-atom with respect to the reference system. The factor σ characterizes the circular polarization state of the light.

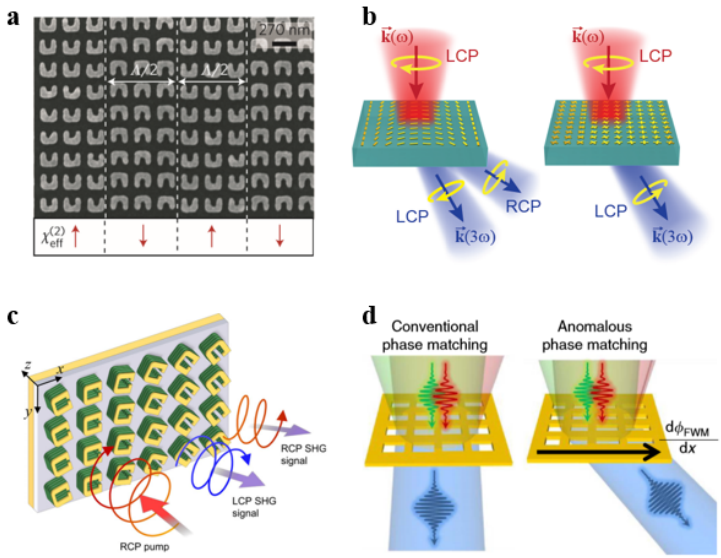

Figure 4| Phase controlled nonlinear metasurface. a, Nonlinear photonic metasurface consisting of split ring resonator meta-atoms (ref. 45). The arrangement in supercells with different orientation (phase shift of π) leads to a phase matching of the SHG light at a defined diffraction angle. b, THG from a nonlinear metasurface based on geometric Berry phase meta-atoms (adapted from ref. 117). The spatially variant orientation results in a continuous phase gradient of for the THG signal that leads to a deflection of the nonlinear beam. c, Metal-Quantum well hybrid metasurface exhibiting a Pancharatnam-Berry phase for SHG (ref. 118). The coupling to intersubband transitions results in a strongly increased nonlinear efficiency of the SHG process. d,

Phase control of FWM in plasmonic metasurfaces by tailoring the resonance condition of inversed meta-atoms (ref. 119).

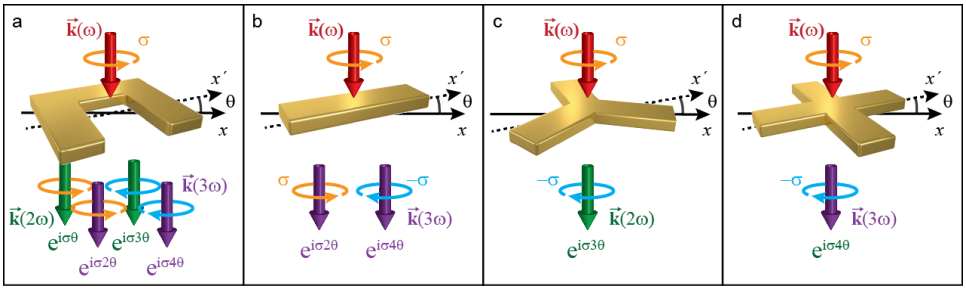

Figure 5| Nonlinear Geometric Phase Elements. a-d, Nonlinear phase elements with one-, two-, three- and four-fold rotational symmetry (C1-C4). The nonlinear geometric Berry phases with a phase of $(n\text{-}1)\sigma\theta$ or $(n\text{+}1)\sigma\theta$ for the n^{th} harmonic generation of the fundamental wave. Based on the symmetry, only particular nonlinear processes and polarization states are allowed. a, The relative phase of the SHG (n=2) from a C1 symmetric meta-atom is θ and 3θ; the relative phase of THG is 2θ and 4θ. b, SHG from a C2 symmetric structure is forbidden, hence leading only to a relative phase for the THG is 2θ and 4θ. c, For a C3 meta-atom the THG is forbidden, the relative phase of SHG with opposite circular polarization is 3θ. d, SHG from C4 meta-atom is forbidden, the relative phase of the THG with opposite circular polarization is 4θ.

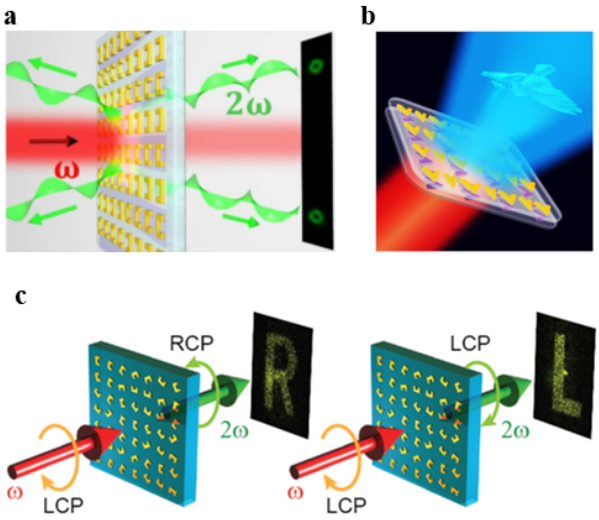

Figure 6| Nonlinear beam shaping and holography. a, Diffraction of SHG signals from a metasurface made of SRR meta-atoms. With the orientation of the SRRs, a discrete phase in the nonlinear material polarization of 0 and π can be introduced (ref.

137). b, Nonlinear holography with SHG on V-shaped meta-atoms using the abrupt phase change due to different resonance conditions (ref. 139). c, Nonlinear metasurface hologram for circularly polarized light. The local Berry phase in the nonlinear polarization results from orientation of SRRs. This technique allows the encoding of different images into one metasurface as the two opposite polarization states corresponding to different phases (adapted from ref. 140).

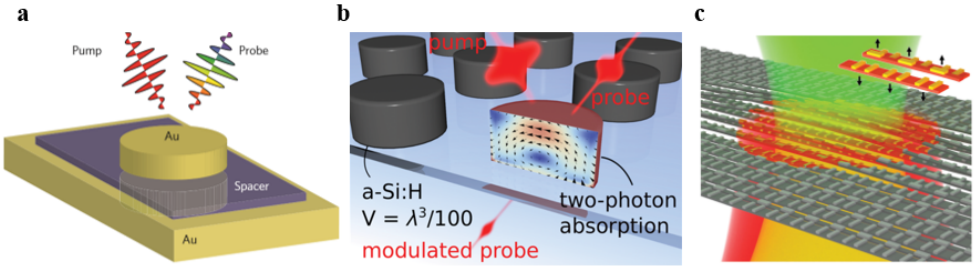

Figure 7| Nonlinear metamaterial and metasurfaces for optical switching and modulation. a, The all-optical ultrafast response can be controlled by tailoring the excitation of hot electrons on plasmonic metasurface (ref. 157). b, All-optical ultrafast switching by using enhanced two photon absorption in silicon metasurface (ref. 162). c, All-optical modulation from giant nano-optomechanical nonlinearity in plasmonic metamaterial (ref. 167).